

Research Article

Poly I:C and STING agonist-primed DC increase lymphoid tissue polyfunctional HIV-1-specific CD8⁺ T cells and limit CD4⁺ T-cell loss in BLT mice

Marta Calvet-Mirabent^{#1,2}, Daniel T. Claiborne^{#3}, Maud Deruaz^{#4,5}, Serah Tanno^{3,4}, Carla Serra⁶, Cristina Delgado-Arévalo^{1,2}, Ildelfonso Sánchez-Cerrillo¹, Ignacio de los Santos⁷, Jesús Sanz⁷, Lucio García-Fraile⁷, Francisco Sánchez-Madrid^{1,2}, Arantzazu Alfranca¹, María Ángeles Muñoz-Fernández⁸, Todd M. Allen³, Maria J. Buzón⁶, Alejandro Balazs^{3,4}, Vladimir Vrbnac^{##3,4} and Enrique Martín-Gayo^{##1,2} 

¹ Immunology Unit, Instituto de Investigación Sanitaria Princesa, Hospital Universitario de la Princesa, Madrid, Spain

² Medicine Department, Universidad Autónoma of Madrid, Madrid, Spain

³ Ragon Institute of MGH, MIT and Harvard, Cambridge, Massachusetts, USA

⁴ Human Immune System Mouse Program, Massachusetts General Hospital, Boston, Massachusetts, USA

⁵ Center for Immunology and Inflammatory Diseases, Massachusetts General Hospital, Boston, Massachusetts, USA

⁶ Infectious Diseases Department, Hospital Universitari Vall d'Hebron, Institut de Recerca (VHIR), Universitat Autònoma de Barcelona, Catalonia, Spain

⁷ Infectious Diseases Unit, Instituto de Investigación Sanitaria Princesa, Hospital Universitario de la Princesa, Madrid, Spain

⁸ Immunology Section, Instituto Investigación Sanitaria Gregorio Marañón (IiSGM), Hospital General Universitario Gregorio Marañón, Madrid, Spain

Effective function of CD8⁺ T cells and enhanced innate activation of DCs in response to HIV-1 is linked to protective antiviral immunity in controllers. Manipulation of DC targeting the master regulator TANK-binding Kinase 1 (TBK1) might be useful to acquire controller-like properties. Here, we evaluated the impact of the combination of 2'3'-c'diAM(PS)2 and Poly I:C as potential adjuvants capable of potentiating DC's abilities to induce polyfunctional HIV-1 specific CD8⁺ T-cell responses *in vitro* and *in vivo* using a humanized BLT mouse model. Adjuvant combination enhanced TBK-1 phosphorylation and IL-12 and IFN- β expression on DC and increased their ability to activate polyfunctional HIV-1-specific CD8⁺ T cells *in vitro*. Moreover, higher proportions of hBLT mice vaccinated with ADJ-DC exhibited less severe CD4⁺ T-cell depletion following HIV-1 infection compared to control groups. This was associated with infiltration of CD8⁺ T cells in the white

Correspondence: Dr. Enrique Martín-Gayo
e-mail: enrique.martin@uam.es

[#]These authors have contributed equally to the study.

^{##}These authors share senior authorship.

pulp from the spleen, reduced spread of infected p24⁺ cells to LN, and with preserved abilities of CD8⁺ T cells from the spleen and blood of vaccinated animals to induce specific polyfunctional responses upon antigen stimulation. Therefore, priming of DC with PolyI:C and STING agonists might be useful for future HIV-1 vaccine studies.

Keywords: CD8⁺ T cell · dendritic cell · hBLT mouse · lymphoid tissue · vaccine



Additional supporting information may be found online in the Supporting Information section at the end of the article.

Introduction

A remaining challenge to end the HIV-1 pandemic is the development of an effective vaccine capable of providing protective and long-lasting immunity against HIV-1 infection. While previous efforts to achieve this goal have failed [1, 2], the scientific community has come to understand that the induction of effective and durable HIV-1-specific T-cell responses in different anatomical compartments will most likely require the targeting and fine-tuning of specific innate immune cell subsets such as DCs. DCs play a critical role during the priming of specific adaptive immune responses, since they are capable of both efficiently presenting Ags to T cells and also mediating the polarization of effector lymphocytes [3, 4]. In fact, DC-based therapeutic vaccines have shown very promising results in clinical trials for cancer therapy [5]. However, although encouraging, previous DC-based HIV-1 vaccination strategies have demonstrated limited abilities priming durable memory HIV-1-specific T-cell responses [6–9]. In addition, most vaccine studies used adjuvants administered systemically to globally increase innate immune activation, without considering their individual impact on specific DC functional characteristics [10].

Previous studies showed that conventional DC (cDC) from HIV-1 elite controllers (EC) are capable of efficiently detecting HIV-1 reverse transcripts [11, 12] and inducing activation of the signal transducer TANK-binding Kinase 1 (TBK1) [13, 14]. This mechanism leads to enhanced capabilities to prime polyfunctional HIV-1-specific CD8⁺ T-cell responses, which are associated with effective control of HIV-1 infection [15, 16]. Therefore, TBK1 may, in principle, represent a therapeutic target to improve DC maturation toward an EC-like phenotype and to more efficiently activate protective antiviral CD8⁺ T-cell responses in a broader population of individuals. Combined stimulation of DC with ligands to multiple intracellular sensors upstream TBK1, such as cGAS, RIG-I, MDA5, or TLR3 [17], could be used as adjuvants to maximize TBK1 activation and further improve the function of these cells. Supporting this possibility, initial studies suggested that the maturation of DC in the presence of the TLR3/RIG-I ligand Poly I:C boosts HIV-1-specific T-cell responses from HIV-1-infected individuals *in vitro* [18]. Multiple vaccine studies have mainly focused on analyzing activation patterns on circulating HIV-1-specific T cells, despite growing evidence of the critical role of lymphoid tissue-resident T cells controlling HIV-1 or SIV [19, 20].

Therefore, it is critical to determine the efficiency and relevance of potential novel DC-based vaccine strategies inducing HIV-1-specific adaptive immune responses *in vivo* in different tissue locations.

The nonhuman primate model has been traditionally recognized as the gold standard *in vivo* model to test HIV-1 vaccine candidates [21]. However, in addition to intrinsic differences with the human organism, this *in vivo* model might not always be accessible for initial phases of vaccine candidate evaluation. Immunodeficient NOD/SCID IL2Ry^{-/-} (NSG) mice transplanted with human fetal HSCs, liver, and thymus (hereafter referred to as hBLT-mouse) represent a more accessible humanized *in vivo* system that recapitulates the development of most human myeloid and lymphoid lineages that has been useful to study HIV-1 pathology [22–26]. Importantly, hBLT-mice can be infected with HIV-1 and meet some aspects of HIV-1 disease progression, such as the depletion of CD4⁺ T lymphocytes and the induction of specific adaptive immune responses including cytotoxic CD8⁺ T cells [27, 28]. Moreover, the hBLT model supports the induction of effector memory HIV-1-specific CD8⁺ T cells similar to those observed in previous vaccine studies [29, 30]. Despite some limitations, the hBLT mouse represents a very attractive model for a proof-of-concept of HIV-1 vaccine study. Recent data indicate that the immunization of hBLT mice with HIV-1 Gag protein potentiates the induction of Gag-specific T cells capable of reducing HIV-1 viremia and forcing viral escape mutations [31]. However, whether the hBLT model supports the induction of protective T-cell responses in different lymphoid tissue compartments that could actively contribute to viral control after vaccination has not been studied in detail. In addition, little, if any, information on the polyfunctional characteristics of CD8⁺ T cells, a critical hallmark of immune control of HIV-1 infection [32, 33], has been described in this system. Finally, the impact and potential benefits of a DC-based HIV-1 vaccine on the induction of HIV-1 specific T cells and disease progression have not been tested in the hBLT mouse model yet.

In this study, we assessed the ability of DC primed with Poly I:C and 2'3'-c'diAM(PS)2 adjuvants (ADJ) to improve parameters of immune protection against HIV-1 in the lymphoid tissue and peripheral blood using the hBTL mouse model. Our data indicate that ADJ-treated DC loaded with Gag peptides potentiate the infiltration of CD8⁺ T cells in the white pulp of spleen and the accumulation of infected HIV-1 p24⁺ cells in these areas,

preventing viral spread to secondary lymphoid organs. These histological parameters induced by GAG-ADJ-DC-vaccination correlated with preserved abilities to induce polyfunctional CD8⁺ T-cell responses in the spleen upon HIV-1 Gag stimulation and with less severe depletion of CD4⁺ T cells at late time points of infection in vaccinated hBLT mice. Our study provides novel evidence of enhanced cellular immunity against HIV-1 in the lymphoid tissue induced by a vaccine based on DC primed simultaneously with Poly I:C and 2'3'-c'diAM(PS)2 *in vivo*, which could be useful for future new vaccine strategies.

Results

Combination of TBK1 adjuvants improves maturation and functional properties of DC

We first evaluated the efficacy of TLR3 and STING agonists Poly I:C and 2'3'-di-AM(PS)2 as potential adjuvants enhancing TBK1 activation, maturation, and functional properties of DCs. To this end, we stimulated monocyte-derived DC (MDDC) and primary circulating CD11c⁺ cDCs with these molecules individually or in combination and monitored the phosphorylation of TBK1 and the downstream effector IRF3 as a readout of activation. As shown in Fig. 1A and Supporting Information Fig. S1A, stimulation of both MDDC and cDC with a combination of the STING agonist and Poly:IC (from hereafter referred to ADJ) led to a more significant increase in TBK1 and IRF3 phosphorylation compared to individual treatments. Therefore, simultaneous stimulation with the STING agonist and Poly I:C could have a significant impact on the activation and subsequent maturation of DC. To test this, we assessed the transcription of mRNAs encoding inflammatory cytokines on primary cDCs and MDDC stimulated with TBK1 adjuvants. We observed that ADJ cocktail induced significantly higher transcriptional levels of IFN- β and IL-12 mRNAs in both DC subtypes although transcriptional levels of these cytokines tended to be higher on cDCs (Fig. 1B). Therefore, these data suggested that our adjuvant combination enhanced the maturation program of DC. To test this, we assessed the expression of maturation markers on ADJ-primed cDC by flow cytometry. As shown in Supporting Information Fig. S1B, both STING agonist and Poly I:C were able to significantly increase the expression of CD40 and CD86 individually, and the combination of both adjuvants led to limited but significant additional increase in the expression of CD40. Moreover, cDC treated with the ADJ combination could induce higher proportions of CD8⁺ T cells coexpressing IFN- γ and the degranulation marker CD107a, suggesting improved functional APCs function (Supporting Information Fig. S1C). Importantly, treatment of PBMC from healthy donors with our ADJ cocktail and a pool of HIV-1 Gag peptides subsequently boosted with autologous cDC treated under the same conditions enhanced *de novo* induction of IFN- γ ⁺ HIV-1 Gag-specific CD8⁺ T cells *in vitro* (Fig. 1C, Upper panel). Moreover, significantly higher proportions of polyfunctional HIV-1-specific IFN- γ ⁺ CD8⁺ T coexpressing CD107a were detected in the presence of cDC loaded with Gag-peptides and stimulated with the ADJ cocktail (Fig. 1C,

lower panel). Importantly, these effects were dependent on the presence of the Ag since no significant increase of T-cell responses was observed after stimulation only with adjuvants (Supporting Information Fig. S1D). Together, these data suggest that combination of Poly I:C and 2'3'-di-AM(PS)2 STING agonist efficiently activate TBK1 and can be used as adjuvants to potentiate the maturation and function of both cDCs and MDDC *in vitro*.

Vaccination of hBLT-mice with ADJ-primed DC reduces HIV-1-mediated disease progression

We next determined whether DC preactivated in the presence of the ADJ cocktail could also enhance effective immune responses against HIV-1 infection *in vivo* using the hBLT mouse model. To ensure that only DCs were manipulated with our adjuvant combination, we differentiated CD11c⁺ CD14⁻ HLADR⁺ cDC and CD11c⁺ CD14⁺ HLADR⁺ MoDC-like cells *in vitro* from a portion of the human fetal CD34⁺ HSC precursors used to reconstitute the hBLT mice prior to vaccination (Supporting Information Fig. S2A). HSC-derived cDC and MoDC were sorted and cultured separately for 24 h in the presence of media alone (MED), a pool of HIV-1 Gag peptides alone (GAG), or in combination with our ADJ cocktail (GAG-ADJ) (Supporting Information Fig. S2B and C). The individual addition of Gag peptides did not induce significant activation of sorted cells. However, despite differences in basal expression of activation markers, both sorted DC subsets responded to the adjuvant stimulation (Supporting Information Fig. S2C) and cells from each condition were pooled for vaccination. In two experiments performed with different batches of hBLT mice, a total of n = 42 hBLT animals were subdivided in three groups of n = 14 animals that were vaccinated intravenously with either MED, GAG, or GAG-ADJ DC by injection in the tail vein. Two weeks after vaccination, mice were intravenously infected with 10,000 TCID₅₀ of JRCF HIV-1 strain (Supporting Information Fig. S2D). Prior pilot experiments indicated that HIV-1 plasma viremia begins to stabilize by 3 weeks postinfection (p.i.) and reaches a stable setpoint by 6 weeks p.i. in hBLT (Supporting Information Fig. S2E). In addition, it has been reported that at 6 weeks p.i. depletion of CD4⁺ T cells and disease progression reproducibly becomes more evident in hBLT mice infected with JRCF HIV-1 [27] and is the peak time point of detection of HIV-1 specific T-cell responses in the blood of these animals [31]. Therefore, we analyzed clinical, histological, and cellular parameters associated with protection or disease progression at 3, 5 or 6, and 6 or 7 weeks p.i. to cover these critical time points (Supporting Information Fig. S2D). As shown in Supporting Information Fig. S2F, no differences in weight were observed among the three hBLT mouse groups prior or after HIV-1 infection, suggesting vaccination did not have any significant impact on the induction of GvHD. Although all hBLT mouse groups experienced a significant reduction in circulating hCD4⁺ T cells 3 weeks after infection with HIV-1 compared to baseline, we observed a noticeably less severe CD4⁺ T-cell depletion in the GAG-ADJ group at 5/6 weeks p.i. (Fig. 2A; Supporting Information Fig. S3A). Notably, the GAG-ADJ vaccinated group included a significantly higher proportion

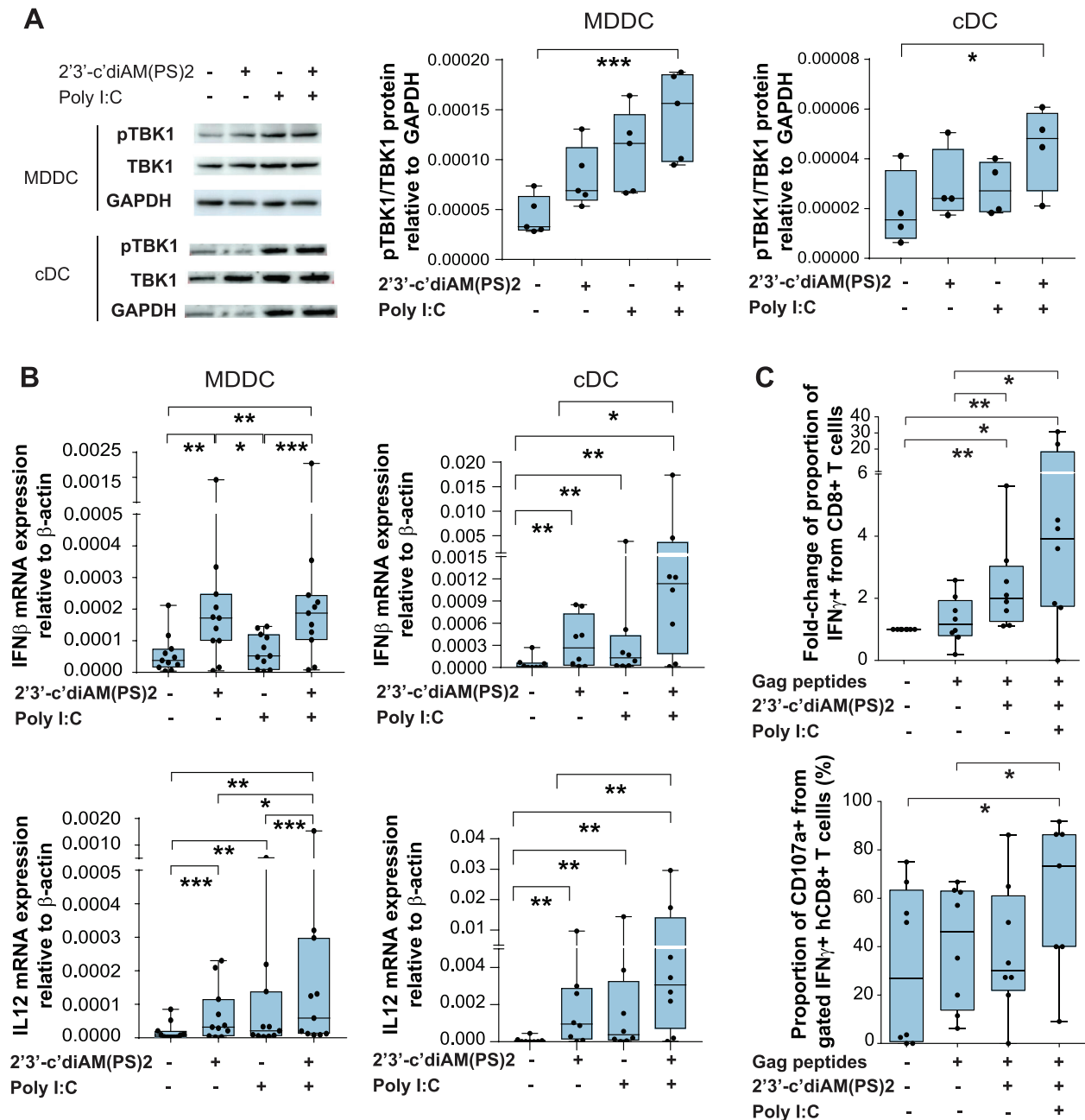


Figure 1. Impact of combined Poly I:C and 2'3'-c-di-AM(PS)2 STING agonist enhancing TBK1 activation and functional maturation of DC in vitro. (A) Representative Western blot of phosphorylated and total TBK1 proteins in monocyte-derived DC (MDDC) and primary DC (cDC) cultured in the absence or the presence of the indicated adjuvants (left panel). Activation of TBK1 protein as a ratio of phosphorylated versus total protein normalized to GAPDH as housekeeping protein for MDDCs (middle plot; $n = 5$ independent experiments) or cDCs (right plot; $n = 4$ independent experiments). Statistical significance was calculated using a Friedman multiple comparison test with Dunn's correction ($*p < 0.05$; $***p < 0.001$). (B) RT-qPCR analysis of IFN- β (upper plots) and IL-12 (lower plots) mRNA expression normalized to β -actin levels in MDDCs (left plots; $n = 11$ independent experiments) or cDCs (right plots; $n = 8$ independent experiments) cultured for 16 h with media alone or in the presence of 2'3'-c-di-AM(PS)2 and/or Poly I:C. Statistical significance was calculated using a two-tailed matched-pairs Wilcoxon test ($*p < 0.05$; $**p < 0.01$; $***p < 0.001$). (C) Proportions of *de novo* induced total (IFN- γ^+ , left) and polyfunctional (IFN- γ^+ CD107a $^+$, right) HIV-1-Gag-specific CD8 $^+$ T cells from total PBMCs obtained from healthy donors ($n = 8$ independent experiments). Significance was calculated using a two-tailed Wilcoxon test ($*p < 0.05$; $**p < 0.01$).

of animals experiencing less than 0.5-fold reduction in circulating CD4 $^+$ T-cell numbers (CD4 $^{\text{Hi}}$ phenotype) at these late time points (Fig. 2A). In contrast, the majority of mice vaccinated with GAG DC experienced a dramatic depletion of CD4 $^+$ T cells below 0.5-

fold threshold (CD4 $^{\text{Lo}}$ phenotype) (Fig. 2A). Interestingly, mice vaccinated with MED DCs were characterized by an intermediate phenotype of 50% animals exhibiting dramatic (<0.5-fold decrease) and 50% less severe (>0.5-fold decrease) depletion

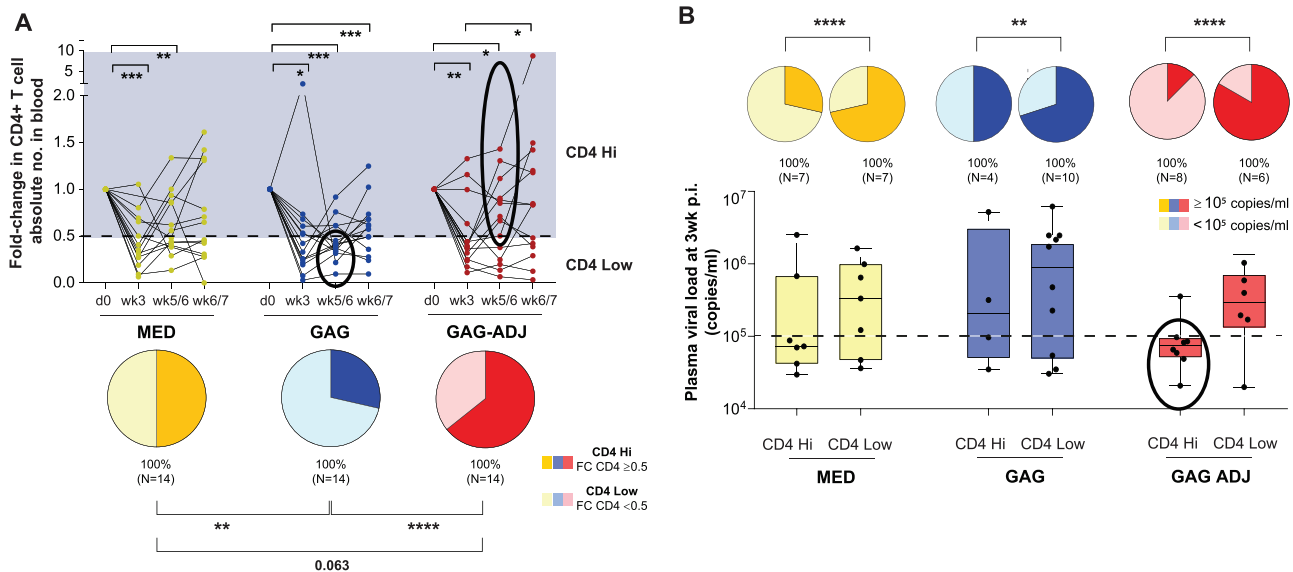


Figure 2. hBLT mice vaccinated with GAG-ADJ DC display less severe progression of HIV-1 infection. (A) Fold-change in circulating hCD4 T-cell counts in infected hBLT mice from basal counts at day 0 to 3, 5 or 6, and 6 or 7 weeks postinfection with HIV-1. Pie charts showing percentage of mice displaying less severe decrease of hCD4 T-cell counts (hCD4 T-cell fold-change ≥ 0.5 ; CD4 Hi) and severe depletion (hCD4 T-cell fold-change < 0.5 ; CD4 Low). Statistical significance of a two-tailed Wilcoxon test ($*p < 0.05$; $**p < 0.01$; $***p < 0.001$) and a Chi-square test with Yates correction ($**p < 0.01$; $****p < 0.0001$). (B): HIV-1 plasma viral loads (lower panels) of hBLT-mice vaccinated with MED, GAG, and GAG-ADJ treated DCs at 3 weeks postinfection, stratified by CD4 Hi and CD4 low phenotypes within each indicated hBLT mouse subgroup. Pie charts (upper panels) representing proportions mice stratified by CD4 T-cell fold-change presenting VLs either equal or higher (dark color) or lower than 10^5 copies/mL (light color) within each treatment group. Statistical significance of differences was calculated using a Chi-square test with Yates correction ($**p < 0.01$; $****p < 0.0001$). (A-B): $n = 14$ pooled mice from each group were analyzed including $n = 8$ and $n = 6$ mice for two different animal batches.

of CD4⁺ T cells, suggesting a partial and Ag-independent effect of vaccination with immature DC (Fig. 2A). Similar but less significant results were obtained at 6 or 7 weeks p.i. (Fig. 2A). Consistently, CD4⁺/CD8⁺ T-cell ratio in the blood tended to be higher in GAG-ADJ mice at later time points of infection (Supporting Information Fig. S3A and B). Furthermore, we observed that those hBLT mice displaying a less severe CD4Hi phenotype were characterized by significantly lower plasma HIV-1 viral loads at 3 weeks p.i., and this pattern was more significantly enriched in the GAG-ADJ and MED animal groups (Fig. 2B). No significant differences were observed in plasma viral loads by 5 or 6 and 6 or 7 weeks p.i., suggesting an early but transient control of viremia in vaccinated mice (Supporting Information Fig. S3C and D). These data indicate that vaccination of hBLT mice with TBK1-trained DC is associated with less severe depletion of CD4⁺ T cells and a concomitant partial early control of HIV-1 viremia, suggesting delayed progression of HIV-1 infection in these animals.

Accumulation of CD8⁺ T cells and HIV-1-infected cells in the spleen white pulp after vaccination with GAG-ADJ-DC

To better understand differences in HIV-1 disease progression in the three groups of vaccinated hBLT mice, we analyzed histological distribution of CD8⁺ T cells and infected p24⁺ cells by immunofluorescence in tissue sections from spleen from the hBLT mice at 6 or 7 weeks p.i. As shown in Fig. 3A and Sup-

porting Information Fig. S4B, p24⁺ HIV-1-infected cells could be detected in the spleen of all hBLT mice, consistent with previous observations [27]. Remarkably, significantly higher numbers of CD8⁺ T cells infiltrated the spleen white pulp areas as defined by H & E staining (Supporting Information Fig. S4A and B), from GAG-ADJ vaccinated hBLT mice at 6 or 7 weeks p.i. (Fig. 3A and B left panel). Moreover, increased infiltration of CD8⁺ T cells in the white pulp was significantly associated with the expression of Granzyme B in the spleen (Fig. 3B, right panel). Additionally, we observed significantly increased proportions of Granzyme B⁺ cytotoxic CD8⁺ T cells in the surrounding red pulp areas in the spleen of GAG-ADJ mice, which also correlated with infiltration of Granzyme B⁺ CD8⁺ T cells in the white pulp (Supporting Information Fig. S4C). Interestingly, CD8⁺ T cells infiltrating the spleen white pulp also tended to express higher levels of Granzyme B and CXCR5 in GAG-ADJ mice, while CXCR5⁺ CD8⁺ T cells were generally less observed in GAG mice in these areas (Supporting Information Figs. S4C and S5A and B). Moreover, significantly higher ratios of CXCR5⁺ CD8⁺ T cells were detected in the white pulp *versus* surrounding red pulp areas in the GAG-ADJ mice group, compared to the GAG group (Supporting Information Fig. S5B, right panel). In contrast, no significant differences in detection of CXCR5⁺ CD3⁺ CD8⁻ Tfh-like cells were observed in the white pulp areas between animal groups (Supporting Information Fig. S5C). Notably, we also observed a significantly higher accumulation of p24⁺ cells in white pulp areas of spleen from these GAG-ADJ hBLT mice compared to those vaccinated with GAG, which was correlated with increased infiltration of

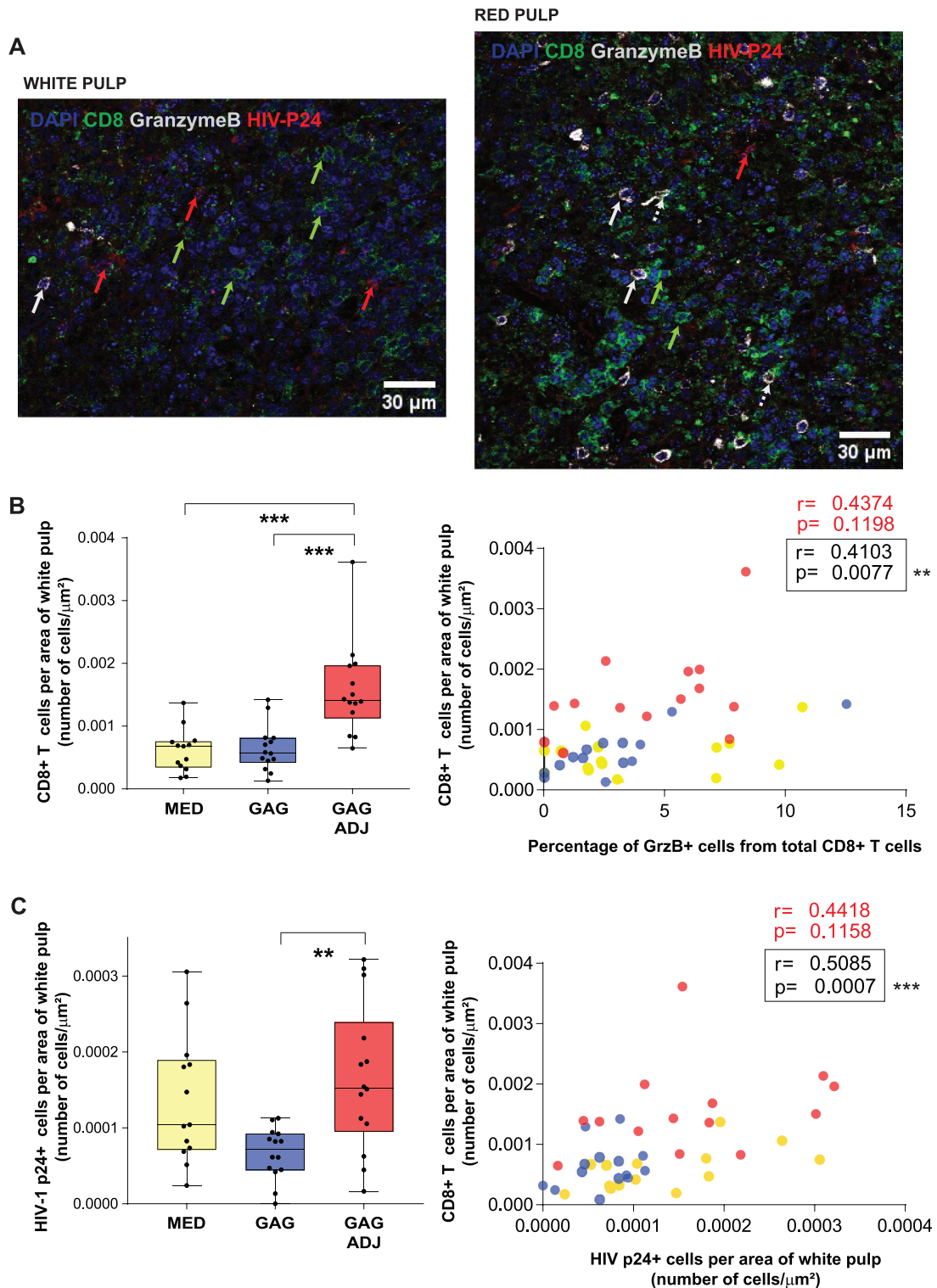


Figure 3. Histological analysis of CD8⁺ T cell and HIV-1-infected cell distribution in spleen from vaccinated hBLT mice. (A) Zoomed images (40 \times magnification) from selected white pulp and red pulp areas defined as in Supplemental Fig. 4, of a transversal splenic section showing staining of cell nuclei (DAPI; blue), human CD8⁺ T cells (green), Granzyme B⁺ (gray), and HIV-1 p24⁺-infected cells (red). Green arrows highlight CD8⁺ T cells; white arrows highlight Granzyme B⁺ cell; dashed white arrows highlight Granzyme B⁺ CD8⁺ T cells; red arrows highlight HIV-1 p24⁺ cells. (B-C): Analysis of hCD8⁺ T cells (B, left) and HIV-1 p24⁺ cells (C, left) infiltrated in the white pulp areas from spleen of the indicated mice groups. For each vaccine group, n = 14 mice were pooled, including n = 8 (MED n = 7) and n = 6 mice, from two animal batches. Significance was calculated using a Kruskal-Wallis multiple comparison test with Dunn's correction (** $p < 0.01$; *** $p < 0.001$). Spearman correlation analysis of association of frequencies of CD8⁺ T cells in the white pulp with proportions of Granzyme B⁺ CD8⁺ T cells (B, right) and p24⁺ in the white pulp (C, right) are also shown. Spearman R and P values are highlighted on the upper right areas of each plot.

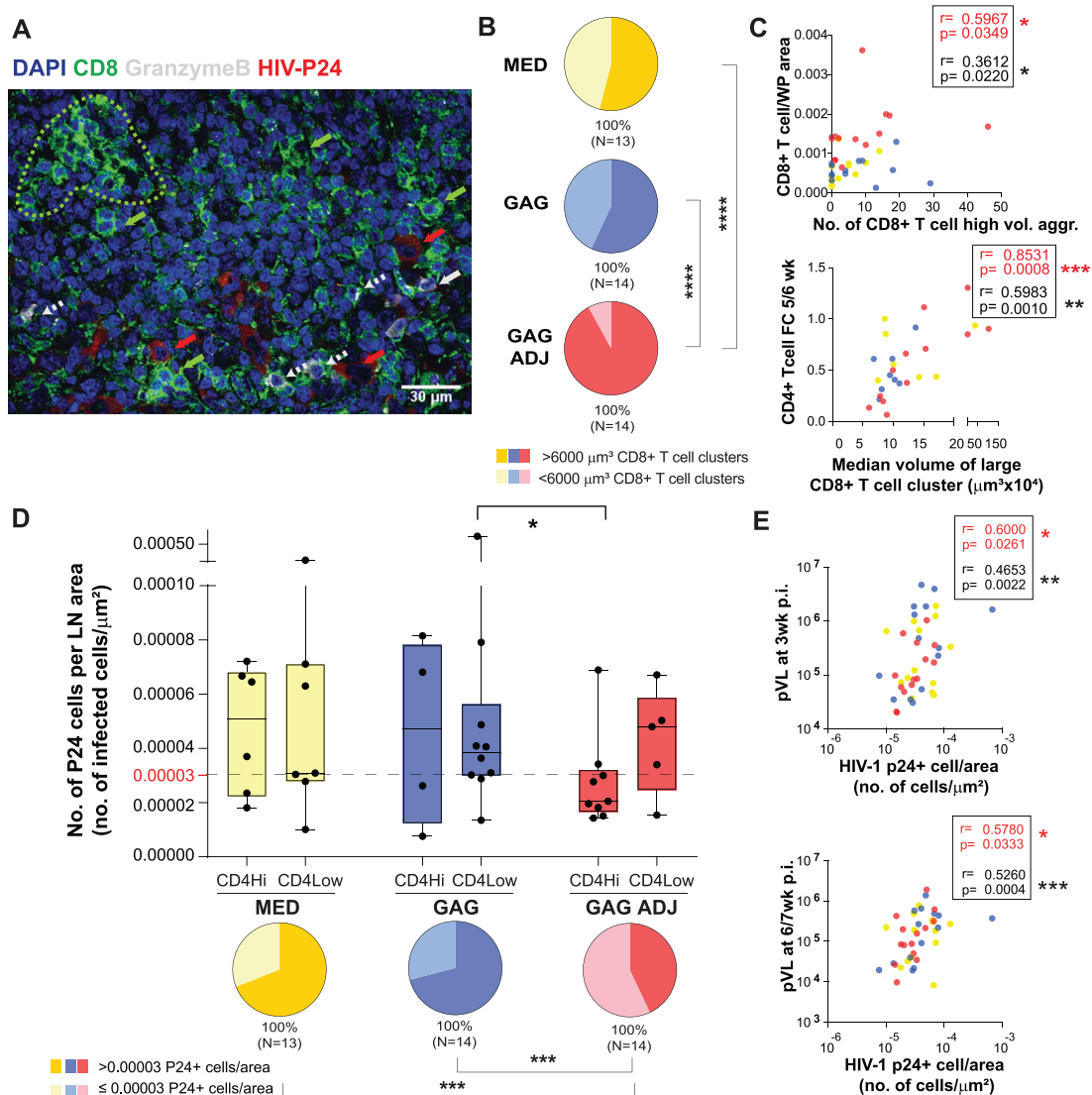


Figure 4. Histological CD8⁺ T cell and HIV-1 p24⁺ cell characterization in LNs from vaccinated hBLT mice. (A) A zoomed area of a representative confocal microscopy LN section (40 \times magnification) showing staining of nuclei (DAPI, blue), hCD8⁺ T cells (green), Granzyme B⁺ (grey), and infected HIV-1 p24⁺ cells (red). Dashed lines highlight CD8⁺ T-cell cluster areas. Green arrows highlight CD8⁺ T cells; white arrow highlights Granzyme B⁺ CD8⁻ cell; dashed white arrows highlight Granzyme B⁺ CD8⁺ T cells; red arrows highlight HIV-1 p24⁺ cells. (B) Percentage of mice presenting CD8⁺ T cells large volume clusters (≥ 6000 cubic microns) in the lymph nodes corresponding to the quantifications shown in Supporting Information Fig. 6. Statistical significance of differences was calculated using a Chi-square test with Yates correction (**** $p < 0.0001$). (C) Individual Spearman correlations between CD8⁺ T-cell clusters (≥ 6000 cubic microns) versus the indicated parameters. Spearman R and p values for all animals (black) and GAG-ADJ group (red) are shown on each plot. (D) Numbers of infected HIV-1 p24⁺ cells per LN area stratified by CD4 Hi and CD4 low animals included on each hBLT mouse subgroup. Pie charts showing percentage of mice displaying high density (≥ 0.00003 p24⁺ cells/ μm^2) or low density of infected cells per area (< 0.00003 p24⁺ cells/ μm^2) within each hBLT mouse subgroup. Significance was calculated using a two-tailed unpaired Mann-Whitney test ($*p < 0.05$; $**p < 0.01$; $***p < 0.001$) and Chi-square test with Yates correction (**** $p < 0.0001$). (E) Individual Spearman correlations of p24⁺ cells per LN area versus plasma viral loads at different time points. Values of r and p in all (black) and GAG-ADJ (red) hBLT mice are highlighted on each plot ($*p < 0.05$; $**p < 0.01$; $***p < 0.001$). (B-E) $n = 14$ pooled mice from each group were analyzed including $n = 8$ ($n = 7$ for MED) and $n = 6$ mice for two animal batches.

CD8⁺ T cells in this area (Fig. 3C). Finally, these observed histological patterns on the spleen did not seem to be associated with differential detection of HLA-DR^{hi} myeloid cells in this organ at 6 or 7 weeks p.i. (Supporting Information Fig. S5D). Together, these data indicate an increased cytotoxic state of CD8⁺ T cells in the spleen and higher infiltration in the white pulp associates with concentration of HIV-1-infected p24⁺ cells in these areas in GAG-ADJ hBLT mice.

Reduced spread of HIV-1 infection to LNs in hBLT mice vaccinated with GAG-ADJ-DC

We next studied whether the histological patterns present in the spleen of GAG-ADJ mice could also be associated with differential distribution of CD8⁺ T cells and HIV-1-infected cells in other lymphoid tissues such as the LN. Notably, CD8⁺ T cells present in the LN from GAG-ADJ vaccinated hBLT animals distributed in

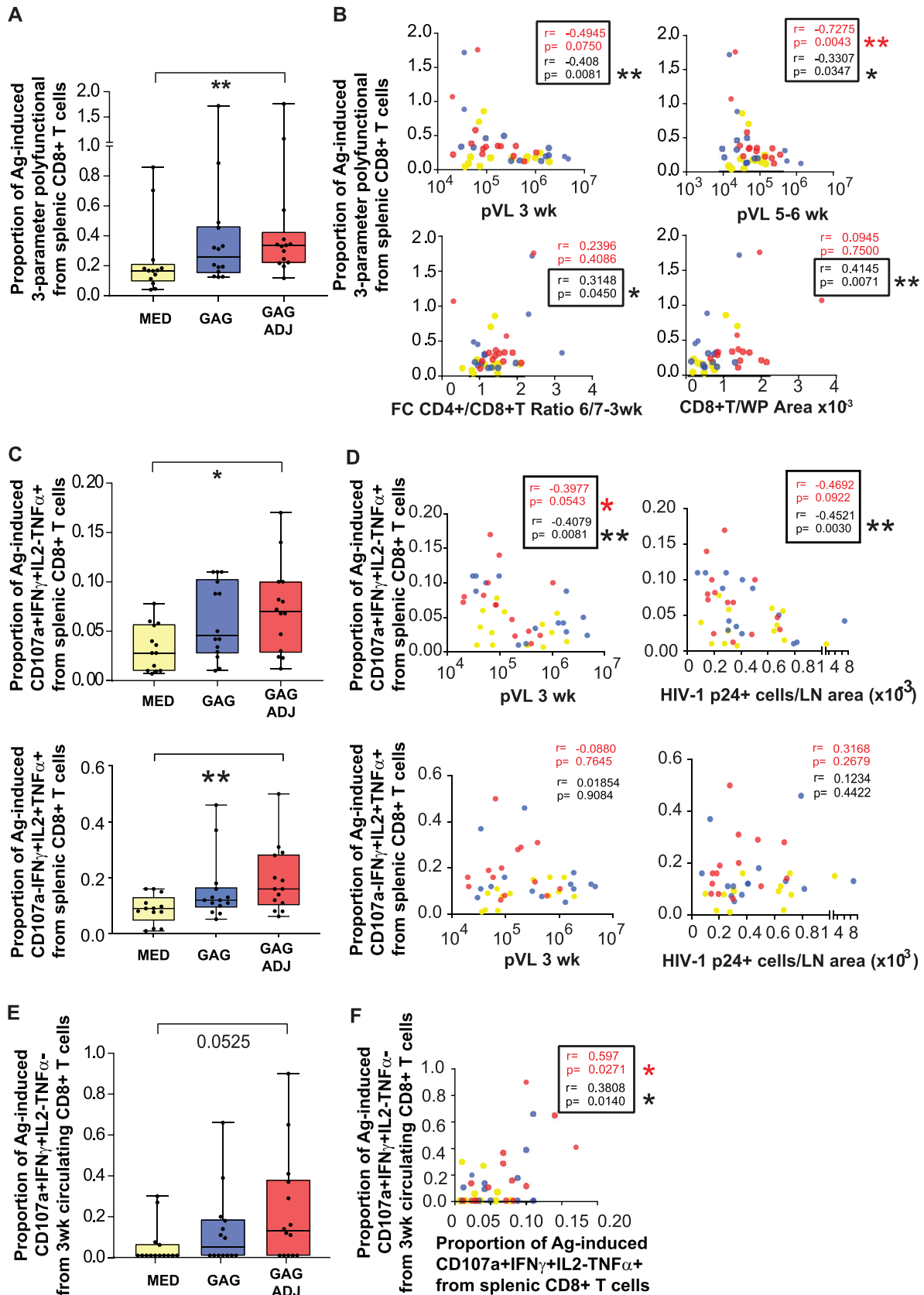


Figure 5. Identification of polyfunctional CD8⁺ T cell patterns associated with histological and clinical parameters of progression of HIV-1 infection in hBLT mice. (A): Proportion of splenic CD8⁺ T cells coexpressing three out of four tested cytokine/degranulation parameters upon stimulation

significantly larger cell clusters (Fig. 4A and B, Supporting Information Fig. S6A and B). Granzyme B tended to be more frequently detected in CD8⁺ T cells in proximity to infected p24⁺ cells rather than in clustered CD8⁺ T cells (Fig. 4A, Supporting Information Fig. S6A). Importantly, larger CD8⁺ T-cell aggregation patterns were positively correlated with increased recruitment of CD8⁺ T cells into the white pulp areas of the spleen and with less severe depletion of CD4⁺ T cells at 5 or 6 weeks p.i., suggesting that they could be associated with delayed disease progression (Fig. 4C and Supporting Information Tables S1 and S2). Although detection of HIV-1 p24⁺ cells was generally lower in LNs compared to the spleen in all groups at 6 or 7 weeks p.i., these infected cells were reduced in GAG-ADJ hBLT mice and more significantly in animals from this group experiencing less severe depletion of CD4⁺ T cells compared to CD4^{Low} GAG-mice (Fig. 4A and D). On the other hand, higher numbers of p24⁺ cells per LN area correlated with viral load detection either at 3 weeks p.i. or 6–7 weeks p.i. (Fig. 4E) and were inversely associated with CD8⁺ T-cell recruitment in the spleen and larger CD8⁺ T-cell clusters in the LN (Supporting Information Tables S1 and S2). However, aggregation of CD8⁺ T cells in the LN did not appear to be associated with differential detection of CXCR5⁺ CD8⁺ T cells or Tfh-like (CXCR5⁺ CD3⁺ CD8⁻) cells in these organs. Similarly, although HLA-DR^{Hi} myeloid cells appeared to be more detectable in LN compared to spleen, no obvious differences were observed between mice from different vaccine groups (Supporting Information Fig. S6C and D). Together, our data indicate that vaccination of hBLT mice with ADJ-trained DC increases specific histological patterns of infiltrated CD8⁺ T-cell responses and accumulation of HIV-1-infected cells in the spleen are interconnected with reduced spread and progression of HIV-1 infection in peripheral organs from these mice.

Polyfunctional HIV-1-specific CD8⁺ T-cell responses in lymphoid tissue and blood from hBLT mice vaccinated with GAG-ADJ-DC

We next addressed the polyfunctional profiles of splenic and circulating CD8⁺ T cells from the three vaccinated hBLT mouse groups by analyzing the expression of IFN- γ , IL-2, TNF- α , and CD107a after *ex vivo* culture in media or stimulation with a pool of HIV-1 Gag peptides at 3 and 6 or 7 weeks p.i. We analyzed the

proportions of T cells coexpressing 2, 3, and 4 of the analyzed parameters as a readout for polyfunctionality and quantified all individual cell subsets by Boolean gating. Using this strategy, we observed a gradual increase in basal and Gag-peptide-induced polyfunctional responses in circulating CD8⁺ T cells at 6 or 7 weeks p.i. from MED to GAG and GAG-ADJ vaccinated hBLT mice (Supporting Information Fig. S7A and B). Moreover, we observed a significant increase in the proportions of three-parameter polyfunctional CD8⁺ T cells present in the spleen in GAG-ADJ hBLT mice after Gag peptide stimulation (Fig. 5A). Importantly, significant associations were found between proportions of splenic antigen-mediated polyfunctional CD8⁺ T cells coexpressing three parameters with increased infiltration of CD8⁺ T cells in the white pulp areas from the spleen and clinical parameters associated with less severe disease progression such as lower plasma viremia at 3 and 5 or 6 weeks p.i, increased ratio of CD4⁺/CD8⁺ T-cell ratios in the blood at 6 or 7 weeks compared to 3 weeks (Fig. 5B; Supporting Information Tables S1 and S2). We next asked which specific populations of three-parameter polyfunctional CD8⁺ T cells from the spleen more significantly contributed to the mentioned observations. From the four possible subsets potentially affected, we observed a more significant increase in the proportion of CD107a⁺IFN- γ ⁺IL-2⁻TNF- α ⁺ and CD107a⁻IFN- γ ⁺IL-2⁺TNF- α ⁺ CD8⁺ T cells, while the other combinations did not reach significance (Fig. 5C, Supporting Information Fig. S7C). Interestingly, we observed that of these two Ag-induced polyfunctional T-cell subsets, only the population of CD107a⁺IFN- γ ⁺IL-2⁻TNF- α ⁺ CD8⁺ T cells significantly correlated with histological and clinical parameters of delayed progression such as lower plasma viral load at 3 weeks p.i. ($p = 0.0081$), lower detection of p24⁺-infected cells in the LN ($p = 0.0030$), higher infiltration of CD8⁺ T cells in the spleen ($p = 0.0010$), and with higher CD4⁺/CD8⁺ T-cell ratios in the blood ($p = 0.0468$) (Fig. 5D; Supporting Information Fig. S7D; Tables S1 and S2).

Finally, we asked whether preserved polyfunctional responses after antigen stimulation from circulating cells at an earlier time-point of infection could predict clinical or histological patterns observed in hBLT mice vaccinated with GAG-ADJ-DC. Interestingly, we found that a polyfunctional CD107a⁺IFN- γ ⁺IL-2⁻TNF- α ⁻ cell population induced by Gag peptide stimulation from circulating CD8⁺ T cells at 3 weeks p.i. was more significantly increased in GAG-ADJ hBLT mice (Fig. 5E). Although propor-

with a pool of HIV-1 Gag peptides. Significance was calculated using a Kruskal–Wallis multiple comparison test with Dunn’s correction (** $p < 0.01$). (B) Individual Spearman correlations between proportions of Gag-peptide induced splenic CD8⁺ T cells coexpressing three cytokine/degranulation parameters and the indicated clinical and histological parameters. Spearman p and r values are highlighted in each plot (* $p < 0.05$; ** $p < 0.01$). (C): Splenic polyfunctional T-cell population defined as CD107a⁺ IFN γ ⁺ IL-2⁻ TNF α ⁺ (upper plot) and CD107a⁻ IFN γ ⁺ IL-2⁺ TNF α ⁺ (lower plot) detected upon stimulation with a pool of HIV-1 Gag peptides. Significance was calculated using a Kruskal–Wallis multiple comparison test with Dunn’s correction (* $p < 0.05$; ** $p < 0.01$). (D): Individual Spearman correlations between proportions of each splenic polyfunctional population *versus* plasma viral load at 3 weeks p.i. (left plots) or HIV-1 p24⁺ cells detected per LN area (right plots). Spearman p and r values are highlighted in each plot in black for all mice and red for the GAG-ADJ group (* $p < 0.05$; ** $p < 0.01$). (E): Proportions of CD107a⁺ IFN- γ ⁺ TNF- α ⁻ IL-2⁻ from circulating CD8⁺ T cells at 3 weeks p.i. after HIV-1 Gag-peptide stimulation. Significance was calculated using a Kruskal–Wallis multiple comparison test with Dunn’s correction (* $p < 0.05$; ** $p < 0.01$). (F): Individual Spearman correlations between proportions of this population and Ag-induced three parameter polyfunctional cells. Significance was calculated using a Kruskal–Wallis multiple comparison test with Dunn’s correction (* $p < 0.05$; ** $p < 0.01$). (A–F): $n = 14$ pooled mice from each group were analyzed including $n = 8$ ($n = 7$ for MED) and $n = 6$ mice for two different animal batches.

tions of circulating CD107a⁺IFN- γ ⁺IL-2⁻TNF- α ⁻ T cells were not directly associated with any clinical and histological parameters (Supporting Information Fig. S7D), this subset significantly correlated with subsequent increased proportions of splenic Ag-induced CD107a⁺IFN- γ ⁺IL-2⁻TNF- α ⁺ observed at 6 or 7 weeks p.i. (Fig. 5F). Together, our results indicate that vaccination of hBLT mice with ADJ-trained DC enhance Ag-inducible precursors of polyfunctional T-cell responses on circulating cells that could serve as biomarkers of tissue polyfunctionality and reduced progression of HIV-1 infection.

Discussion

Our study evaluates the efficacy of simultaneous maturation of DC with STING agonist and PolyI:C agonist increasing activation of TBK1 and functional parameters in these cells, as an adjuvant strategy to improve DC-based vaccination and enhance immune responses against HIV-1 *in vivo*. We demonstrate that vaccination with ADJ-primed DC is associated with reduced spread of HIV-1 infection and less severe CD4⁺ T-cell depletion in hBLT mouse model. Previous clinical trials evaluated the benefits of systemic administration of PolyI:C to HIV-1-infected individuals, and demonstrated an increase of HIV-1-specific T-cell responses but the therapeutic benefits of this format remain unclear [34–36]. In addition, while previous studies in a murine model suggested that HIV-1 vaccines administered systemically targeting DC via CD40 or DEC205 and PolyI:C as an adjuvant could induce antigen-specific responses [37–39], our work provides new proof-of-concept of beneficial effects of the administration of a combination of adjuvants potentiating TBK1 activation directly on DC *in vitro* and as a vaccine in an *in vivo* humanized model without systemic adjuvant addition, which can trigger other cell populations. This is particularly relevant since it has been shown that systemic Poly I:C administration can lead to HIV-1 reactivation on CD4⁺ T cells [38, 40]. Moreover, this study specifically explores the benefits of enhanced maturation of DC in the presence of a combination of PolyI:C and STING agonist, potentiating phosphorylation of TBK1 and IRF3, and more efficiently inducing the secretion of immunomodulatory cytokines, such as IL-12 and IFN- β , which were associated with an increase of DC-antigen presenting properties. However, we cannot completely rule out that in addition to activating TBK1, some of the adjuvants used in our study, such as PolyI:C, could be also triggering additional pathways, which might also affect DC maturation. Despite this possibility, our data indicate that our combined adjuvant strategy is able to recapitulate some of the enhanced functional properties previously observed in DC from HIV-1 ECs [11, 41]. In addition, we have provided proof-of-concept that combination of PolyI:C and 2'3'di (AM)PS2 STING agonist enhances *de novo* priming of polyfunctional HIV-1-specific T cells after a first round of stimulation of PBMC with this adjuvant combination thereby potentiating APC function and a subsequent boost with autologous DC treated with the same agonists. Further studies are required to determine whether stimulation of naïve T cells with consecutive cocultures

with autologous GAG-ADJ DC would be sufficient to visualize *de novo* priming of HIV-1-specific responses *in vitro*. Furthermore, our data suggest that our adjuvant combination might trigger different functional characteristics in different cDCs and Mo-derived DC subtypes such as the efficiency in inducing proinflammatory cytokines or the expression of costimulatory molecules. For this reason, we decided to use both DC subtypes in our *in vivo* experiments. However, these potential differences should be taken into account for future vaccination designs.

Importantly, while previous studies on HIV-1 vaccine prototypes have mainly focused on the phenotype or even polyfunctionality induced circulating T cells [42], we were able to identify cellular and histological parameters associated with reduced spread of HIV-1 infection to the LN such as the spleen and the LNs. Moreover, vaccination of hBLT mice with GAG-ADJ-primed DC induced higher levels of infiltration of CD8⁺ T cells in white pulp areas of spleen, which was associated with accumulation of infected HIV-1 p24⁺ cells in these areas. This splenic phenotype was associated with higher volume of CD8⁺ T-cell clusters and lower detection of infected cells in the LN of hBLT mice, suggesting a potential control of viral spread in different lymphoid tissues. However, potential differences in kinetics of spread of infected cells to these areas or in their intrinsic abilities to home to these tissues should be investigated in more detail in the hBLT model. Interestingly, the observed histological splenic patterns bear some resemblance to follicular CD8⁺ T-cell responses observed in primates able to control viral infection [20] and in HIV-1 controller patients [19]. In fact, we observed the expression of CXCR5 preferentially on CD8⁺ T cells infiltrating the white pulp areas from GAG-ADJ hBLT mice, which might support a follicular-like phenotype previously linked to viral control [43, 44]. However, since deficiencies in lymphoid tissue architecture have been described in the hBLT model [27, 45], further characterization of CD8⁺ T-cells infiltrating into the white pulp and in the LN in the hBLT mouse needs to be conducted to better understand these potential similarities. In fact, in our study, we did not address the causal relationships between the enrichment in cytotoxic CD8⁺ T cells in the red pulp and the infiltration of CXCR5⁺ CD8⁺ T cells in the white pulp and the differential accumulation of HIV-1 p24⁺ cells observed in these areas. Likewise, further studies are required to better understand associations between detection of clustering of CD8⁺ T cells, expression of CXCR5, and differential detection of p24⁺ in the LN. Also, none of the differential histological patterns observed in the lymphoid tissue from GAG-ADJ mice were associated with detection of myeloid HLA-DRhi cells in the spleen and LN of these animals at 6 or 7 weeks p.i. However, considering the number of weeks since DC vaccination, additional analyses at earlier time points should be performed to better establish connections between myeloid cells and CD8⁺ T cells in lymphoid tissue of these animals. In addition, no obvious differences between vaccine groups were found in detection of CXCR5⁺ CD3⁺ CD8⁻ T cells which could represent Tfh-like cells in the spleen or the LN. Previous studies suggested that Tfh and B-cell maturation are not properly induced in the hBLT mouse [46] and further studies are needed to test whether DC-vaccination could restore their functional abilities to

support B-cell maturation and induce more effective immunoglobulin responses. Furthermore, the relationship between the observed histological distribution of splenic CD8⁺ T cells with specific polyfunctional phenotypes and inflammatory tissue fibrosis, previously linked to immunopathology of HIV-1 infection, was not addressed in our study and deserves further investigation [47, 48]. In addition, our study did not directly address whether increased accumulation of p24⁺-infected cells and CD8⁺ T cells in the white pulp in the GAG-ADJ-DC vaccinated mice could be associated with differences in immune exhaustion or cytotoxic function. However, our data show that CD8⁺ T cells present in white and red pulp areas express higher levels of Granzyme B, which might indicate preserved cytotoxic function in these cells. Finally, it is important to note that the mentioned protective histological patterns identified in our study were not restricted to hBLT mice vaccinated the GAG-ADJ DC, but frequencies of animals capable of developing this particular histological characteristics and delayed HIV-1 progression were more represented in this group.

In addition to histological patterns, we identified in vaccinated hBLT mice preserved abilities of splenic CD8⁺ T cells to induce a polyfunctional population of CD107a⁺ IFN- γ ⁺ TNF- α ⁺ IL-2⁻ cells upon Ag stimulation that was associated with less severe depletion of circulating CD4⁺ T cells, higher infiltration of CD8⁺ T cells in the white pulp areas, and lower numbers of infected p24⁺ cells in the LN, thus, underscoring that these cells could display effective antiviral properties. Supporting this possibility, a number of studies have described that polyfunctional T cells co-expressing TNF- α with other parameters correlate with protection against viral infections such as Zika and Cytomegalovirus [49, 50]. However, whether the precursor of these polyfunctional cells present in the lymphoid tissue derive from tissue-resident cells or from cells preferentially migrating to this anatomical location was not addressed in our study. Thus, future studies are needed to better understand the developmental kinetics and functional relationships of this particular subset of polyfunctional cells with other subpopulations that might also be present in the GAG-ADJ hBLT mice. While our data also indicate that vaccination with DC primed with PolyI:C and 2'3'-c'diAM(PS)2 adjuvants could induce transient control on plasma viral load at early time points, these effects could be mediated by HLA-variability or HIV-1 escape mutations induced in vaccinated hBTL mouse [28, 31]. In addition, another limitation of our study was the relatively high TCID₅₀ dose and the administration route of HIV-1 to the hBLT mice studied, which makes it difficult to evaluate potential physiological differences in plasma viral loads at later time points after infection. To address this possibility in more detail, further studies performed in more physiological model of mucosal infection and with lower viral titers are needed. Although our study suggests that TBK-1 DC can induce multiple histological and immunological parameters that might in principle be associated with immune control of HIV-1 infection, we focused on analyzing them at key time points previously described to mark HIV-1 pathogenesis and detection of HIV-1 responses in the blood. However, a limitation of our study is a week of lag between the first and second mice batches in the intermediate (weeks 5 and

6) and late time points (weeks 6 and 7) used for clinical analysis and to end our in vivo experiments, which caused a partial overlap that may have introduced confounders that could have affected our ability to detect more significant differences in these time points. Despite these limitations, we were able to detect consistent differences across our vaccine arms at the mentioned time point of analysis. Thus, further longitudinal studies with a larger number of hBLT mice and a broader range of time point analyses are required to better establish the impact and evolution of the identified histological and immunological parameters during the course of HIV-1 infection and their relationship with protection.

Finally, the primary objective of our study was to address whether vaccination of mice with ADJ-primed DC could induce some level of protection against progression of HIV-1 infection in a model in which we ensured infection of all mice. However, although we showed a partial delay on some clinical parameters associated HIV-1 progression, such as CD4⁺ T-cell depletion and transient control of viral load, new studies are required to evaluate the beneficial effect and translational potential of modified protocols using single or multiple time point vaccination with ADJ-primed DC prior to infection under more physiological conditions such as the use of lower viral titers and a mucosal or intrasplenic administration routes. Despite these limitations, our study provides evidence of the beneficial effect of ADJ-primed DC inducing more effective immune responses against HIV-1 at the histological, clinical, and cellular levels, and therefore, it may be useful for the development of future vaccine strategies against HIV-1.

Materials and methods

Isolation of human peripheral blood populations

Human PBMCs were isolated by Ficoll (Pancoll, PAN Biotech) gradient centrifugation. Subsequently, cDC and total T cells were purified from PBMC suspensions by negative immunomagnetic selection (purity > 90%) using the Human Myeloid DC Enrichment Kit (STEMCELL) and the Untouched total human T cell (Invitrogen) kits, respectively. MDDC were generated from adherent cells present in PBMCs and cultured in the presence of 100 IU/mL of GM-CSF and IL-4 (Preprotech) for 5 days.

In vitro functional assays

Human PBMCs or purified primary cDCs were cultured in RPMI 1640 media supplemented with 10% Fetal Bovine Serum (HyClone) alone or in the presence of either 1 μ g/mL 2'3'-c'diAM(PS)2 (Invivogen), or 5 μ g/mL Poly I:C (SIGMA), or a combination of both for 24 h. For all functional assays, stimulated cDCs were washed with 1 \times PBS prior to the experiment. For mixed leukocyte reaction (MLR) assays (n = 6), activated DCs were cocultured with allogenic T cells at a DC:T ratio of 1:2 in 96 round-bottom well plates for 5 days. At day 5, cultured

lymphocytes were restimulated with 0.25 $\mu\text{g}/\text{mL}$ PMA (SIGMA) and ionomycin (SIGMA) for 1 h and cultured for 4 h in the presence of 0.5 $\mu\text{g}/\text{mL}$ Brefeldin A (SIGMA), 0.005 mM Monensin, and 0.2 $\mu\text{g}/\text{mL}$ anti-CD107a-APC antibody. Intracellular expression of INF- γ and CD107a on cultured CD8⁺ and CD4⁺ T cells was then analyzed by flow cytometry adhering to the “Guidelines for the use of flow cytometry and cell sorting in immunological studies” [51]. For the experiments evaluating de novo-priming of HIV-1-specific responses ($n = 8$), total PBMCs from healthy donors were prestimulated with 5 $\mu\text{g}/\text{mL}$ of a pool of 129 overlapping HIV-1 Gag peptides (13–16 mer) (NIH AIDS Reagent Program #11057) in the absence or the presence of the adjuvant combinations previously mentioned and kept in culture in media supplemented with 25 IU/mL IL-2 (Prepotech) for 2 weeks to allow all existing APCs (including cDC, monocytes) to more efficiently present peptides to specific T cells and maximize their activation. Subsequently, cDCs were isolated from PBMCs from the same donor and activated under the same conditions in the absence or presence of a pool of HIV-1 Gag peptides. After 16 h, precultured PBMCs were boosted with isolated and adjuvant-stimulated autologous cDCs were cocultured for additional 16 h in the presence of Brefeldin A, Monensin, and CD107a antibody and analyzed by flow cytometry as previously mentioned. All antibodies used for flow cytometry are listed in Supporting Information Table S3. These assays were performed according to MIATA guidelines.

Western blot analysis

Total protein lysates from MDDC ($n = 5$) and cDC ($n = 4$) cultured for 1 h in the presence of media or individual or combined Poly I:C and 2'3'-c-di AM(PS) agonists were obtained using RIPA buffer containing 1% phosphatase and protease inhibitors (Roche Diagnostics). Subsequently, protein lysates were resolved in a 10% agarose gel with SDS and transferred to a nitrocellulose membrane (Fisher Scientific). Membranes were blocked in 5% BSA v (Sigma-Aldrich) in Tris-buffered saline and incubated overnight with 1:100 dilution of primary anti-TBK1, anti-IRF3, or anti-GAPDH antibodies (Supporting Information Table S3). Then, membranes were incubated for 1 h with the appropriate anti-rabbit or anti-mouse secondary antibodies (Supporting Information Table S3). Protein band intensity was quantified by analyzing chemiluminescence detected using an ImageQuant 800 system (Amersham).

Gene expression validation and RT-qPCR

RNA was isolated from cDC cultured in the absence or the presence of TBK1 adjuvants ($n = 8$) using RNeasy Micro Kit (Qiagen) according to manufacturer instructions. Subsequently, cDNA was synthesized using the Reverse Transcription kit (Promega). Transcriptional levels of IFN- β , IL-12, and TNF- α were analyzed by semiquantitative PCR (SYBR Green assay Go Taq qPCR Master Mix; Promega) with specific primers (Metabion) on an Applied Biosystems StepOne Real-Time PCR system (Applied Biosystems).

Relative gene expression was calculated after normalization to β -actin transcriptional levels.

Generation of humanized BLT-mice

Two different batches of a total of 42 NOD/SCID IL2R- γ -/- (NSG) mice transplanted with human BM, fetal liver, and thymus (BLT-mouse) and fetal CD34⁺ HSCs were generated as previously described [26, 27] at the Human Immune System Core from the Ragon Institute and Massachusetts General Hospital in collaboration with Dr. Vladimir Vrbanac, Dr. Maud Deruaz, and Dr. Alejandro Balazs. Mice were housed in microisolator cages and fed autoclaved food and water at a pathogen-free facility. Human immune reconstitution was monitored for 17 weeks and mice were considered reconstituted with proportions of human CD45⁺ lymphocytes superior to 30%.

DC vaccination and HIV-1 infection of hBLT mice

DCs were generated from the same CD34⁺ HSC precursors used to reconstitute the corresponding batch of hBLT mice in the presence of 100 IU/mL FLT3L, SCF, IL-7, and GM-CSF (Prepotech). After 10 days, cDC (CD14⁺ HLA-DR⁻) and MoDC (CD14⁺ HLA-DR⁺) present in cultures were sorted and incubated in media in the absence (MED mice group, $n = 14$) or in the presence of 5 $\mu\text{g}/\text{mL}$ of the above-mentioned pool of peptides (GAG mice group, $n = 14$) alone or in combination with 1 $\mu\text{g}/\text{mL}$ of 2'3'-c-diAM(PS) and 5 $\mu\text{g}/\text{mL}$ Poly I:C adjuvants (ADJ mice group, $n = 14$). After 24 h, cDC and MoDC from each culture condition were pooled and hBLT mice were intravenously vaccinated in the tail vein with approximately 10^5 total DC per animal, containing both 50% of cDC and 50% of MoDC. Two weeks after vaccination, hBLT mice were infected intravenously with a dose of 10,000 TCID₅₀ of HIV-1_{JR-CSF}. For histological analyses, some unvaccinated uninfected mice were included as controls.

Plasma HIV-1 viral loads were assessed at 3 and 5 or 6 and 6 or 7 weeks p.i. by isolating viral RNA from plasma and quantified by RT-qPCR as previously described [31]. Circulating CD4⁺ T-cell counts were assessed at day 0, 3 weeks, 5 or 6 weeks, and 6 or 7 weeks p.i. by flow cytometry using counting beads (CountBright, ThermoFisher). To avoid excessive blood extraction and potential loss of animals, we limited phenotypical analysis of polyfunctional T-cell responses in blood at 3 and 6 or 7 weeks p.i. (see section of “Analysis of polyfunctional T-cell responses”).

Histological analysis of tissue sections from hBLT mice

Axillary and mesenteric lymph nodes and spleens were collected for all 41 surviving mice and paraffin-embedded and segmented in fragments of 2 μm of thickness in a Leica microtome. Tissue sections deparaffinized, hydrated, and target retrieval were performed with a PT-LINK (Dako) previous to staining.

For paraffin-preserved tissue, we used rabbit anti-human CD8 (Abcam), rabbit anti-human CXCR5 (GeneTex), rabbit anti-

human HLA-DR (Abcam), rat anti-human CD8 (Bio-Rad), rat anti-human Granzyme B (eBioscience), mouse anti-human CD3 (Dako), and mouse anti-HIV-1 P24 (Dako), as primary antibodies; and goat anti-rabbit AF488 (Invitrogen), donkey anti-rat AF594 (Jackson ImmunoResearch) and donkey anti-mouse AF647 (ThermoFisher) as secondary antibodies (Supporting Information Table S3). Images were taken with a Leica TCS SP5 confocal and processed with the LAS AF software. 3-D CD8⁺ T-cell aggregations were analyzed with Imaris 9.1 software. CD8⁺, Granzyme B⁺, CXCR5⁺, CD3⁺, and HIV-1 P24⁺ cell counts and colocalization of some of these markers were analyzed with ImageJ software. In some cases, spleen tissue sections were also stained with H&E to discriminate white (no eosin staining) and red pulp (intense eosin staining) areas containing nucleated cells (hematoxylin stained). Finally, quantification of myeloid cells in spleen and LN from vaccinated mice was based on morphology and high levels of HLA-DR expression.

Analysis of polyfunctional T-cell responses

Blood was extracted from the 42 hBLT mice at 3 and 6 or 7 weeks p.i. and lysed with Red Blood Cell Lysis Buffer (SIGMA). T cells were activated for 1.5 h with 5 μ L/mL of anti-CD28 and anti-CD49d in the presence or absence of 6.4 μ g/mL of a Gag pool of peptides in the presence of 0.5 μ g/mL Brefeldin A, Golgi Plug, and CD107a antibody (see Table 1). After 5 h of incubation, polyfunctionality of T-cell response was assessed by INF- γ , IL-2, TNF- α , and CD107a expression by multicolor flow cytometry panel (all antibodies used are listed in Supporting Information Table S3) in a BD LSR Fortessa Instrument (BD Biosciences). Polyfunctionality was evaluated using Boolean gating obtained with FlowJo version 10 software.

Statistics

Significance of phenotypical and functional differences between paired conditions or different animals were assessed using a Wilcoxon matched-pairs signed-rank test or Mann-Whitney U test, or using a Kruskal-Wallis or Friedman test followed by a Dunn's post-hoc multiple comparison test, as appropriate. Dependence of contingency tables values were calculated with Chi-square statistic. Associations between clinical, histological and phenotypical parameters were calculated using nonparametric Spearman correlation individually between two parameters or using a correlation network. All statistical analyses were performed using the GraphPad Prism 8 Software.

Conflict of Interest: The authors declare no conflict of interest.

Ethics approval statement: The in vivo study was conducted by the Human Immune System Core led by Dr. Vladimir Vrbanc following ethical standards for the treated animals specified in the IACUC protocol (number 2009N000136) approved by

the Massachusetts General Hospital Institutional Animal Care and Use Committee (MGH IACUC) and IRB. These protocols were also approved by the Bioethical committee from Universidad Autónoma de Madrid. In addition, human PBMC samples used in the study were obtained from Buffy coat samples from Centro de Transfusiones de la Comunidad de Madrid, which allows the donation of discarded samples for research through their institutional informed consent and following the Helsinki Declaration.

Author contributions: E.M.G., V.V., D.C., M.D., A.B., M.J.B. developed the research idea and study concept, designed the study and wrote the manuscript.

E.M.G., V.V. supervised the study.

M.C.M., D.C., M.D. and S.T. designed and conducted most experiments and equally contributed to the study.

T.A. and D.C. provided longitudinal VL data evolution in BLT mice from a pilot experiment.

M.C.M. performed the histology staining and the image analysis of tissue sections from the study.

M.D. and D.C. provided critical feedback during experimental design and execution phases of the studies and were directly involved in the experiments.

M.J.B. and C.S. provided reagents and support for the histological analyses performed in the study.

F.S.M., A.A., M.A.M.F., I.D.S., L.G.F. and J.S. provided peripheral blood, reagents and participated on the analysis of the data.

Funding: EMG was supported by the NIH R21 program (R21AI140930), the Ramón y Cajal Program (RYC2018-024374-I), the MINECO/FEDER RETOS program (RTI2018-097485-A-I00), by Comunidad de Madrid Talento Program (2017-T1/BMD-5396), and by Centro de Investigación Biomédica en Red (CIBER) de Enfermedades Infecciosas. M.J.B. is supported by the Miguel Servet program funded by the Spanish Health Institute Carlos III (CP17/00179), the MINECO/FEDER RETOS program (RTI2018-101082-B-100), and Fundació La Marató TV3 (201805-10FMTV3). EMG and MJB are funded by “La Caixa Banking Foundation H20-00218). M.C.M. was also funded by the NIH (R21AI140930). FS-M was supported by SAF2017-82886-R from the Ministerio de Economía y Competitividad and HR17-00016 grant from “La Caixa Banking Foundation. We also would like to thank the NIH AIDS Reagent Program, Division of AIDS, NIAID, NIH for providing HIV-1 PTE Gag Peptide Pool from NIAID, DAIDS (cat #11057) for the study. Finally, the Microscopy Unit from Centro Nacional de Investigaciones Cardiovasculares provided technical support for the microscopy image processing and analysis.

Peer review: The peer review history for this article is available at <https://publons.com/publon/10.1002/eji.202149502>

Data availability statement: The data that support the findings of this study are available from the corresponding author upon reasonable request.

References

- 1 O'Connell, R. J., Kim, J. H., Corey, L. and Michael, N. L., Human immunodeficiency virus vaccine trials. *Cold Spring Harb. Perspect. Med.* 2012. 2: a007351.
- 2 Gray, G. E., Laher, F., Lazarus, E., Ensolli, B. and Corey, L., Approaches to preventative and therapeutic HIV vaccines. *Curr. Opin. Virol.* 2016. 17: 104–109.
- 3 O'Keefe, M., Mok, W. H. and Radford, K. J., Human dendritic cell subsets and function in health and disease. Cellular and molecular life sciences: CMLS. 2015.
- 4 Martin-Gayo, E., Gao, C., Chen, H. R., Ouyang, Z., Kim, D., Kolb, K. E. et al., Immunological fingerprints of controllers developing neutralizing HIV-1 antibodies. *Cell Rep.* 2020. 30: 984–996.e4.
- 5 Bol, K. F., Schreibelt, G., Gerritsen, W. R. and de Vries, I. J., Figdor, C. G., Dendritic cell-based immunotherapy: state of the art and beyond. *Clin. Cancer Res.* 2016. 22: 1897–1906.
- 6 Ide, F., Nakamura, T., Tomizawa, M., Kawana-Tachikawa, A., Odawara, T., Hosoya, N. et al., Peptide-loaded dendritic-cell vaccination followed by treatment interruption for chronic HIV-1 infection: a phase 1 trial. *J. Med. Virol.* 2006. 78: 711–718.
- 7 Kundu, S. K., Engleman, E., Benike, C., Shapero, M. H., Dupuis, M., van Schooten, W. C. et al., A pilot clinical trial of HIV antigen-pulsed allogeneic and autologous dendritic cell therapy in HIV-infected patients. *AIDS Res. Hum. Retroviruses* 1998. 14: 551–560.
- 8 Gandhi, R. T., O'Neill, D., Bosch, R. J., Chan, E. S., Bucy, R. P., Shopis, J. et al., A randomized therapeutic vaccine trial of canarypox-HIV-pulsed dendritic cells vs. canarypox-HIV alone in HIV-1-infected patients on antiretroviral therapy. *Vaccine* 2009. 27: 6088–6094.
- 9 García, F., Climent, N., Guardo, A. C., Gil, C., León, A., Autran, B., Lifson, J. D., Martínez-Picado, J., Dalmau, J., Clotet, B., Gatell, J. M., Plana, M. and Gallart, T., A dendritic cell-based vaccine elicits T Cell responses associated with control of HIV-1 replication. *Science Translational Medicine.* 2013. 5. <http://doi.org/10.1126/scitranslmed.3004682>
- 10 Coelho, A. V., de Moura, R. R., Kamada, A. J., da Silva, R. C., Guimaraes, R. L., Brandao, L. A. et al., Dendritic cell-based immunotherapies to fight HIV: how far from a success story? a systematic review and meta-analysis. *Int. J. Mol. Sci.* 2016. 17: 1985.
- 11 Martin-Gayo, E., Buzon, M. J., Ouyang, Z., Hickman, T., Cronin, J., Pimenova, D. et al., Potent cell-intrinsic immune responses in dendritic cells facilitate HIV-1-specific t cell immunity in HIV-1 elite controllers. *PLoS Pathog.* 2015. 11: e1004930.
- 12 Gao, D., Wu, J., Wu, Y. T., Du, F., Aroh, C., Yan, N. et al., Cyclic GMP-AMP synthase is an innate immune sensor of HIV and other retroviruses. *Science* 2013, 341: 903–906.
- 13 Habjan, M. and Pichlmair, A., Cytoplasmic sensing of viral nucleic acids. *Curr. Opin. Virol.* 2015, 11: 31–37.
- 14 Ma, Z. and Damania, B., The cGAS-STING defense pathway and its counteraction by viruses. *Cell Host & Microbe* 2016. 19: 150–158.
- 15 Almeida, J. R., Price, D. A., Papagno, L., Arkoub, Z. A., Sauce, D., Bornstein, E. et al., Superior control of HIV-1 replication by CD8+ T cells is reflected by their avidity, polyfunctionality, and clonal turnover. *J. Exp. Med.* 2007. 204: 2473–2485.
- 16 Betts, M. R. and Harari, A., Phenotype and function of protective T cell immune responses in HIV. *Curr Opin HIV AIDS* 2008. 3: 349–355.
- 17 Zhao, C. and Zhao, W., TANK-binding kinase 1 as a novel therapeutic target for viral diseases. *Expert Opin. Ther. Targets* 2019. 23: 437–446.
- 18 Huang, X. L., Fan, Z., Borowski, L. and Rinaldo, C. R., Maturation of dendritic cells for enhanced activation of anti-HIV-1 CD8(+) T cell immunity. *J. Leukoc. Biol.* 2008. 83: 1530–1540.
- 19 Nguyen, S., Deleage, C., Darko, S., Ransier, A., Truong, D. P., Agarwal, D. et al., Elite control of HIV is associated with distinct functional and transcriptional signatures in lymphoid tissue CD8(+) T cells. *Sci. Transl. Med.* 2019. 11: eaax4077.
- 20 Fukazawa, Y., Lum, R., Okoye, A. A., Park, H., Matsuda, K., Bae, J. Y. et al., B cell follicle sanctuary permits persistent productive simian immunodeficiency virus infection in elite controllers. *Nat. Med.* 2015. 21: 132–139.
- 21 Sui, Y., Gordon, S., Franchini, G. and Berzofsky, J. A., Nonhuman primate models for HIV/AIDS vaccine development. *Curr. Protoc. Immunol.* 2013. 102: 1–30.
- 22 Lan, P., Tonomura, N., Shimizu, A., Wang, S. and Yang, Y. G., Reconstitution of a functional human immune system in immunodeficient mice through combined human fetal thymus/liver and CD34+ cell transplantation. *Blood* 2006. 108: 487–492.
- 23 Marsden, M. D., Kovochich, M., Suree, N., Shimizu, S., Mehta, R., Cortado, R. et al., HIV latency in the humanized BLT mouse. *J. Virol.* 2012. 86: 339–347.
- 24 Wege, A. K., Melkus, M. W., Denton, P. W., Estes, J. D. and Garcia, J. V., Functional and phenotypic characterization of the humanized BLT mouse model. *Curr. Top. Microbiol. Immunol.* 2008. 324: 149–165.
- 25 Weichseldorfer, M., Heredia, A., Reitz, M., Bryant, J. L. and Latinovic, O. S., Use of humanized mouse models for studying HIV-1 infection, pathogenesis and persistence. *Journal of AIDS and HIV Treatment* 2020. 2: 23–29.
- 26 Strieppecke, R., Münz, C., Schuringa, J. J., Bissig, K. D., Soper, B., Meeham, T. et al., Innovations, challenges, and minimal information for standardization of humanized mice. *EMBO Mol. Med.* 2020. 12: e8662.
- 27 Brainard, D. M., Seung, E., Frahm, N., Cariappa, A., Bailey, C. C., Hart, W. K. et al., Induction of robust cellular and humoral virus-specific adaptive immune responses in human immunodeficiency virus-infected humanized BLT mice. *J. Virol.* 2009. 83: 7305–7321.
- 28 Dudek, T. E., No, D. C., Seung, E., Vrbanc, V. D., Fadda, L., Bhoumik, P. et al., Rapid evolution of HIV-1 to functional CD8(+) T cell responses in humanized BLT mice. *Sci. Transl. Med.* 2012. 4: 143ra98.
- 29 Garcia, F., Lejeune, M., Climent, N., Gil, C., Alcami, J., Morente, V. et al., Therapeutic immunization with dendritic cells loaded with heat-inactivated autologous HIV-1 in patients with chronic HIV-1 infection. *J. Infect. Dis.* 2005. 191: 1680–1685.
- 30 Kloverpris, H., Karlsson, I., Bonde, J., Thorn, M., Vinner, L., Pedersen, A. E. et al., Induction of novel CD8+ T-cell responses during chronic untreated HIV-1 infection by immunization with subdominant cytotoxic T-lymphocyte epitopes. *AIDS* 2009. 23: 1329–1340.
- 31 Claiborne, D. T., Dudek, T. E., Maldini, C. R., Power, K. A., Ghebremichael, M., Seung, E. et al., Immunization of BLT humanized mice redirects T cell responses to Gag and reduces acute hiv-1 viremia. *J. Virol.* 2019. 93.
- 32 Betts, M. R., Nason, M. C., West, S. M., De Rosa, S. C., Migueles, S. A., Abraham, J. et al., HIV nonprogressors preferentially maintain highly functional HIV-specific CD8+ T cells. *Blood* 2006. 107: 4781–4789.
- 33 Migueles, S. A., Laborico, A. C., Shupert, W. L., Sabbaghian, M. S., Rabin, R., Hallahan, C. W. et al., HIV-specific CD8+ T cell proliferation is coupled to perforin expression and is maintained in nonprogressors. *Nat. Immunol.* 2002. 3: 1061–1068.
- 34 Thompson, K. A., Strayer, D. R., Salvato, P. D., Thompson, C. E., Klimas, N., Molavi, A. et al., Results of a double-blind placebo-controlled study

- of the double-stranded RNA drug polyI:polyC12U in the treatment of HIV infection. *Eur. J. Clin. Microbiol. Infect. Dis.* 1996. **15**: 580–587.
- 35 Armstrong, J. A., McMahon, D., Huang, X. L., Pazin, G. J., Gupta, P., Rinaldo, C. R., Jr. et al., A phase I study of ampligen in human immunodeficiency virus-infected subjects. *J. Infect. Dis.* 1992. **166**: 717–722.
- 36 Miller, E., Spadaccia, M., Sabado, R., Chertova, E., Bess, J., Trubey, C. M. et al., Autologous aldrithiol-2-inactivated HIV-1 combined with polyinosinic-polycytidylic acid-poly-L-lysine carboxymethylcellulose as a vaccine platform for therapeutic dendritic cell immunotherapy. *Vaccine* 2015. **33**: 388–395.
- 37 Apostólico, J. S., Lunardelli, V. A. S., Yamamoto, M. M., Cunha-Neto, E., Boscardin, S. B. and Rosa, D. S., Poly(I:C) potentiates T cell immunity to a dendritic cell targeted HIV-multiepitope vaccine. *Front. Immunol.* 2019. **10**: 843.
- 38 Cheng, L., Wang, Q., Li, G., Banga, R., Ma, J., Yu, H. et al., TLR3 agonist and CD40-targeting vaccination induces immune responses and reduces HIV-1 reservoirs. *J. Clin. Invest.* 2018. **128**: 4387–4396.
- 39 Gómez, C. E., Nájera, J. L., Sánchez, R., Jiménez, V. and Esteban, M. Multimeric soluble CD40 ligand (sCD40L) efficiently enhances HIV specific cellular immune responses during DNA prime and boost with attenuated poxvirus vectors MVA and NYVAC expressing HIV antigens. *Vaccine* 2009. **27**: 3165–3174.
- 40 Alvarez-Carbonell, D., Garcia-Mesa, Y., Milne, S., Das, B., Dobrowolski, C., Rojas, R. et al., Toll-like receptor 3 activation selectively reverses HIV latency in microglial cells. *Retrovirology* 2017. **14**: 9.
- 41 Martin-Gayo, E., Cole, M. B., Kolb, K. E., Ouyang, Z., Cronin, J., Kazer, S. W. et al., A reproducibility-based computational framework identifies an inducible, enhanced antiviral state in dendritic cells from HIV-1 elite controllers. *Genome Biol.* 2018. **19**: 10.
- 42 Lévy, Y., Thiébaud, R., Montes, M., Lacabartz, C., Sloan, L., King, B. et al., Dendritic cell-based therapeutic vaccine elicits polyfunctional HIV-specific T-cell immunity associated with control of viral load. *Eur. J. Immunol.* 2014. **44**: 2802–2810.
- 43 He, R., Hou, S., Liu, C., Zhang, A., Bai, Q., Han, M. et al., Follicular CXCR5-expressing CD8(+) T cells curtail chronic viral infection. *Nature* 2016. **537**: 412–428.
- 44 Leong, Y. A., Chen, Y., Ong, H. S., Wu, D., Man, K., Deleage, C. et al., CXCR5(+) follicular cytotoxic T cells control viral infection in B cell follicles. *Nat. Immunol.* 2016. **17**: 1187–1196.
- 45 Murooka, T. T., Deruaz, M., Marangoni, F., Vrbanc, V. D., Seung, E., von Andrian, U. H. et al., HIV-infected T cells are migratory vehicles for viral dissemination. *Nature* 2012. **490**: 283–287.
- 46 Karpel, M. E., Boutwell, C. L. and Allen, T. M., BLT humanized mice as a small animal model of HIV infection. *Curr. Opin. Virol.* 2015. **13**: 75–80.
- 47 Zeng, M., Haase, A. T. and Schacker, T. W., Lymphoid tissue structure and HIV-1 infection: life or death for T cells. *Trends Immunol.* 2012. **33**: 306–314.
- 48 Sanchez, J. L., Hunt, P. W., Reilly, C. S., Hatano, H., Beilman, G. J., Khoruts, A. et al., Lymphoid fibrosis occurs in long-term nonprogressors and persists with antiretroviral therapy but may be reversible with curative interventions. *J. Infect. Dis.* 2015. **211**: 1068–1075.
- 49 Giménez, E., Blanco-Lobo, P., Muñoz-Cobo, B., Solano, C., Amat, P., Pérez-Romero, P. et al., Role of cytomegalovirus (CMV)-specific polyfunctional CD8+ T-cells and antibodies neutralizing virus epithelial infection in the control of CMV infection in an allogeneic stem-cell transplantation setting. *J. Gen. Virol.* 2015. **96**: 2822–2831.
- 50 Grifoni, A., Costa-Ramos, P., Pham, J., Tian, Y., Rosales, S. L., Seumois, G. et al., Cutting edge: transcriptional profiling reveals multifunctional and cytotoxic antiviral responses of zika virus-specific CD8(+) T cells. *J. Immunol.* 2018. **201**: 3487–3491.
- 51 Cossarizza, A., Chang, H. D., Radbruch, A., Acs, A., Adam, D., Adam-Klages, S. et al., Guidelines for the use of flow cytometry and cell sorting in immunological studies (second edition). *Eur. J. Immunol.* 2019. **49**: 1457–1973.

Abbreviations: **cDC:** conventional DC · **EC:** elite controller · **GAG:** pool of HIV-1 Gag peptides · **GAG-ADJ:** pool of HIV-1 Gag peptides combined with Poly I:C and STING agonist adjuvants · **MDDC:** monocyte derived-DC · **MED:** media alone, · **MLR:** mixed leukocyte reaction · **p.i.:** postinfection · **TBK1:** TANK-binding Kinase 1

Full correspondence: Enrique Martin-Gayo, Immunology Unit, Medicine Department, Universidad Autónoma de Madrid, Hospital de la Princesa, Calle de Diego de León, 62, 28006 Madrid, Spain.
e-mail: enrique.martin@uam.es

Received: 12/7/2021

Revised: 19/11/2021

Accepted: 14/12/2021

Accepted article online: 22/12/2021